TÜBİTAK

Turkish Journal of Electrical Engineering & Computer Sciences

http://journals.tubitak.gov.tr/elektrik/

Research Article

Turk J Elec Eng & Comp Sci
(2014) 22: 191 – 201
© TÜBİTAK
doi:10.3906/elk-1205-38

Effects of a current transformer's magnetizing current on the driving voltage in self-oscillating converters

Güngör BAL[1], **Selim ÖNCÜ**[2,*]

[1]Department of Electrical and Electronics Engineering, Gazi University, Ankara, Turkey
[2]Department of Electrical and Electronics Engineering, Karabük University, Karabük, Turkey

Received: 14.05.2012 • **Accepted:** 15.10.2012 • **Published Online:** 20.12.2013 • **Printed:** 20.01.2014

Abstract: Magnetizing inductance is one of the parameters that affect the phase and amplitude error of the output current of current transformers (CTs). In this study, the linear circuit model of a CT is developed to be used for driving purposes in power electronics applications. A simulation of the CT and its linear model is achieved. In the model circuit, the effect of the magnetizing inductance on the driving voltage can be examined. The equivalent circuit simulation results and the linear model simulation results along with the calculated results show agreement with each other. These results are compared with experimental results.

Key words: Current transformer, magnetizing current, linear model, self-oscillating drive

1. Introduction

A current transformer (CT) is a special type of transformer that is generally used for stepping down from high current levels to measurable low levels. They are used in high- and low-voltage systems for measuring or surge protection purposes. In addition, they can also be used in power electronics circuits. The output current of CT is converted to the voltage waveform by a burden resistance connected to the secondary side [1]. Therefore, in power circuits, the measurement of the current can be achieved with a lower cost in comparison to Hall-effect sensors [2]. Providing a galvanic isolation, low power losses, operation at a high bandwidth, and sufficient voltage levels for output are the other advantages of CTs [3]. Thus, CTs are broadly used in many applications such as detecting and measuring the current or driving switches based on the current signal [4,5].

In self-oscillating converters, switches can be driven using resonant current or voltage feedback [6]. The switching device, which is powered from a resonant circuit by the current feedback, is called a self-oscillating driver with a CT [7]. The sensitivity levels and power losses of the CT are directly related to its design. Core losses are reduced if cores with high magnetic permeability are used [1]. To increase the sensitivity of the CT, the core should have high magnetic permeability and high resistance [8]. Hence, in the design, toroidal cores, which have a narrow hysteresis curve and do not have an air gap, are generally preferred. A CT's windings can be approximately modeled as a linear coil, as long as the BH curve of the core is linear. Therefore, a linear CT model can be used in the modeling of the system because of its simplicity [3]. In the literature, the linear model was used for electronic ballasts to simplify the gate drive network [5,9–12]. However, the simulation results of both the driver transformer and the linear model with measured parameters and their comparison with experimental results were not presented in those studies.

*Correspondence: soncu@karabuk.edu.tr

In this study, a linear transformer model for different conditions of self-oscillating power converters, which is one of the application areas of CTs, is designed, simulated, and experimentally tested. The output current is converted to voltage form using zener diodes on the secondary side. Hence, a driver circuit model is obtained for voltage controlled switches like MOSFETs. In the model, measured transformer parameters are used. The CT equivalent circuits are achieved with coupled coils and a linear coil. The results for the coupled coils and the linear model are compared. The simulation results of the CT model circuit for different magnetizing currents can be observed. Additionally, the change in the magnetizing current and the effects of this variation to the output voltage can be seen in the simulation circuit simultaneously. The relationship between the secondary current and the output voltage can be observed using the parametric simulation method and the experimental circuit. Boundary conditions for both the magnetizing inductance and the secondary current can be calculated. The measurements taken from the CT show good agreement with the results calculated or obtained from the simulations.

2. Structure of the CT

A typical CT consists of a toroid core with n number of windings and a conductor cable passing through the core. Toroids have the advantage of high efficiency and high magnetic coupling over conventional laminated cores [13] Figure 1 shows the structure and the equivalent circuit of a typical CT. In Figure 1a, the 1-turn conductor, which is placed through the core, is called the primary winding. In Figure 1b, the magnetic coupling between the primary winding and the $n-$turn secondary winding is represented by the coupling factor k.

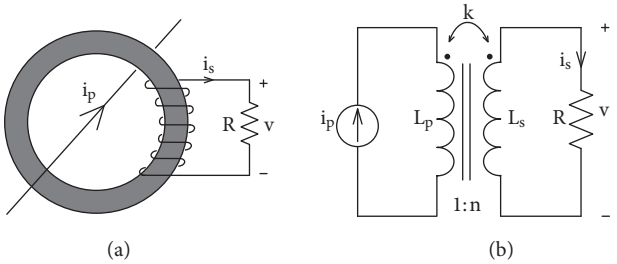

Figure 1. CT: a) construction and b) equivalent circuit.

The output current is converted to a voltage signal with a burden resistance (R) on the secondary side. For 1-turn primary and $n-$turn secondary windings, the secondary current (i_s) can be calculated using the primary (i_p) current and turn number (n) in Eq. (1).

$$i_s = \frac{i_p}{n} \tag{1}$$

In Figure 1b, L_p and L_s are the primary and the secondary winding inductances, respectively.

$$L_p = 1^2 A_L \tag{2}$$

$$L_s = n^2 A_L \tag{3}$$

Here, A_L is the inductance factor of the core and is related to the magnetic permeability and size of the core.

2.1. CT model

In an ideal CT, there are no copper losses or voltage drops. The primary and the secondary currents are in the same phase and they have the ratio obtained from Eq. (1). The linear model of the CT shown in Figure 1 is created with the assumption that the core is not saturated; therefore, the magnetizing inductance is represented by a linear coil [3]. The primary circuit voltage drops, core losses, effects of the winding capacitances, and temperature effects are neglected. With these assumptions, the equivalent circuit of the CT, which is created for the voltage-controlled switches, is shown in Figure 2a. Figure 2b shows the equivalent drive circuit that is reflected on the secondary side with a sinusoidal current source, zener diodes, and CT parameters. In the circuit, zener diodes are used in place of the burden resistance.

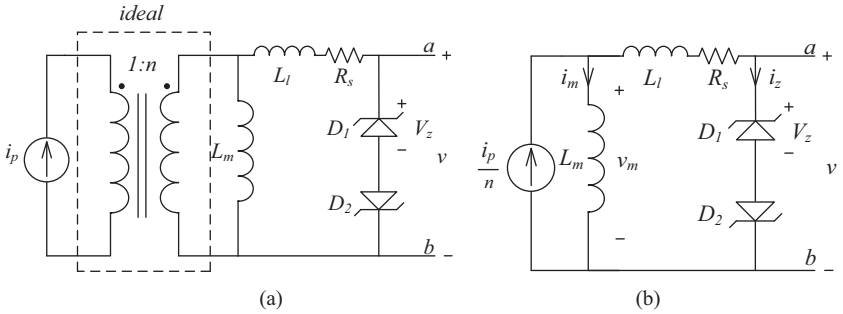

Figure 2. The CT model: a) for the ideal transformer and b) for the equivalent circuit reflected on the secondary side (linear model).

In Figure 2, R_s and L_l are the secondary winding resistance and the leakage inductance, respectively. The parameters of the 1-turn primary winding are not shown in Figure 2 because of its small parameters. L_m is the secondary side magnetizing inductance. L_l can be calculated using the magnetic coupling coefficient (k). If the magnetic coupling between the windings is ideal $(k = 1)$, then the magnetizing inductance is equal to the secondary inductance.

$$L_l = (1 - k) L_s = 0 \tag{4}$$

$$L_m = kL_s = L_s \tag{5}$$

Zener diodes are used in place of the burden resistance in the circuit model, as shown in Figure 2. The output voltage is limited between $+V_z$ and $-V_z$. When the L_m value is sufficient, the i_m current linearly increases or decreases. Figure 3 shows the theoretical current and voltage waveforms of the CT model [10,11].

In self-oscillating power converters, the primary current is converted into a suitable voltage by a CT for driving the switches [12]. The effect of the gate circuit of the power switch is not taken into account in Figure 3. The time delay (t_d) between the secondary current and the driving voltage arises from the effect of the driving circuit parameters. The driving voltage depends on the zener current. If the i_z current is greater than 0, then the output voltage is $+V_z$; otherwise, it is $-V_z$. Therefore, the change in the magnetizing current over time can be defined as in Eq. (6) [3]:

$$i_m(t) = I_O + \frac{1}{L_m} \int_0^{\frac{T_s}{2}} v_m(t)\, dt, \tag{6}$$

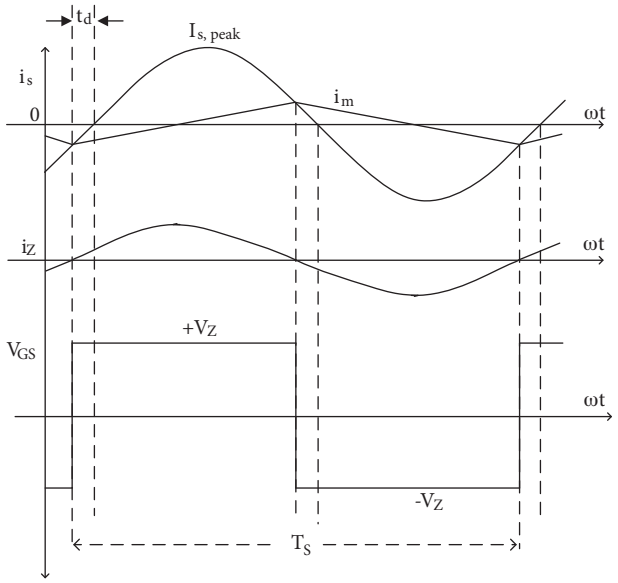

Figure 3. Theoretical waveforms of the CT model.

where I_O is the initial coil current and T_s is the switching period. Because the output voltage is in the square wave form, the approximate peak value of the magnetizing current can be found using the following equation.

$$I_{m,peak} = I_O + \frac{V_z \frac{T_s}{2}}{L_m} \tag{7}$$

The sum of the magnetizing current and the zener current gives the secondary current [10].

$$i_s = i_m + i_z \tag{8}$$

According to Eq. (7), as the L_m value decreases, the magnetizing current increases. The difference between the secondary current and the zener current increases; hence, t_d increases. As a result, the phase difference between the driving voltage and the primary current increases. For this reason, the zener diode voltage, the switching period, and the magnetizing inductance are the parameters that affect the driving voltage.

Obtaining a square wave driving voltage at the circuit depends on the critical magnetizing inductance ($L_{mc??}$). The inductance value has to be above the value given in Eq. (9) for the selected zener voltage and the secondary current.

$$L_{mcr} = \frac{V_z \frac{Ts}{2}}{I_{s,peak}} \tag{9}$$

A situation similar to Eq. (9) also applies to the secondary current. If the $I_{m,peak}$ value reaches the peak secondary current ($I_{s,peak}$) value, the desired square wave output voltage cannot be obtained. For this reason, a turn ratio that would provide currents above the critical secondary current (I_{scr}) value should be selected (Eq. (10)).

$$I_{scr} = I_{m,peak} \tag{10}$$

$$I_{scr} = \frac{V_z \frac{T_s}{2}}{2L_m} \tag{11}$$

2.2. Parameters of the CT

A Philips TN23/14/7 toroid is used for the experimental studies of the CT. The toroid's parameters are given in Table 1 .[14]. A secondary winding is wound on 3 different cores made up of 40, 45, and 50 turns. All of the cores are of the same type. A copper wire with a 0.35-mm diameter is used.

Table 1. Properties of the Philips TN23/14/7 toroid.

$A_L\,(nH)$	$1250 \pm 25\%$
Grade	3F3

The coupling factor between the primary and secondary windings of 1:50 CT is 0.974 when measuring the results over the inductance, capacitance, and resistance (LCR) meter. The coupling factors of the 1:40 and 1:45 transformers are considered as the same as with the 1:50 CT. The calculated parameters of the CTs and their models are given in Table 2.

Table 2. Calculated parameters of the CT.

n (turns)	40	45	50
$L_p\,(mH)$	0.00125	0.00125	0.00125
$L_s\,(mH)$	2	2.531	3.125
$L_m\,(mH)$	1.948	2.465	3.044
$L_l\,(mH)$	0.052	0.066	0.081

3. Simulation and experimental study of the CT

3.1. Linear model

The simulation circuit of the 1:50 CT and its model are set up in PSpice according to the calculated parameters in Table 2. Linear coupled coils are used in Figures 4a and 4b. In these circuits, a current source, which has a 2-A peak value and 40-kHz frequency, is used for the primary current; 15-V zener diodes are selected. Figure 4c shows the simulation circuit of the CT with a linear model. In this circuit, depending on Eq. (1), the peak value of the current source is defined as 40 mA.

The output voltage of the CT and its linear model simulation results are shown in Figure 5, where the CT and its linear model give the same outputs.

The values of the CT parameters measured through the LCR meter are given in Table 3.

Table 3. Measured parameters of the CT.

n (turns)	40	45	50
$L_p\,(mH)$	0.00123	0.00123	0.00123
$L_s\,(mH)$	1.902	2.455	3.120
$R_s\,(\Omega)$	0.5	0.588	0.7

The experimental results are obtained using the 1:50 CT circuit and zener diodes in Figure 6a. Figure 6b gives the experimental output voltage waveform of the 1:50 CT, while the primary current is a 2-A peak at 40 kHz. In the oscilloscope, the current measurements are achieved with a 0.3 Ω/3 W resistance (300 mV = 1 A).

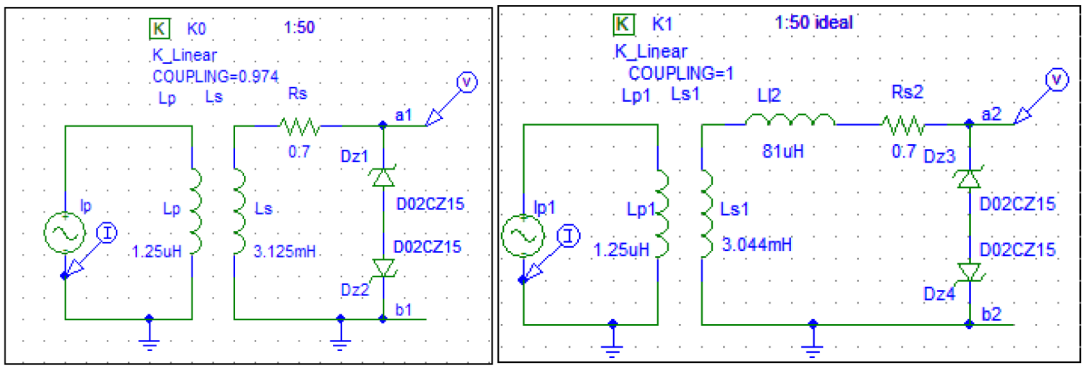

(a) $k = 0.974$ (b) $k = 1$

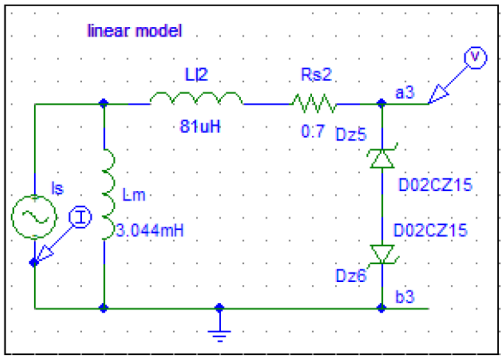

(c) Linear model

Figure 4. Simulation circuit of the CT ($n = 50$).

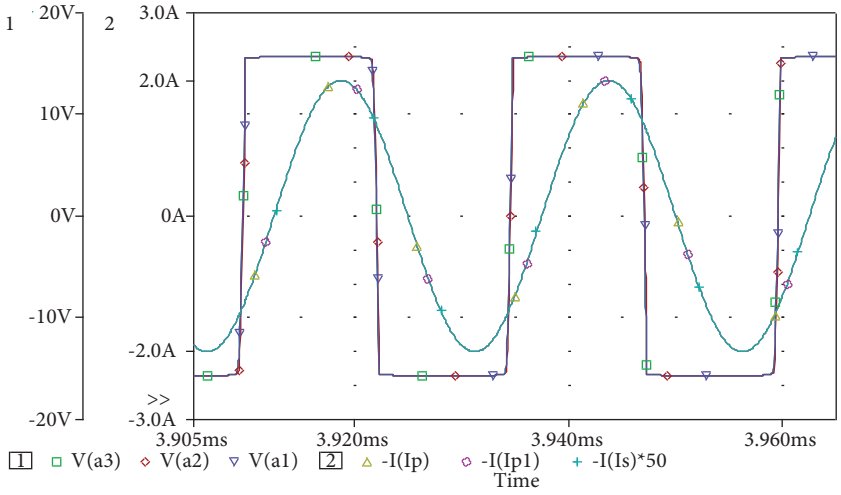

Figure 5. Simulation results of the CT and the linear model.

The simulation and experimental results of the primary and zener diode currents are given in Figures 7a and 7b, respectively. In the simulation results, the magnetizing current is also shown. According to the

waveforms, there is a phase difference between the primary current and the zener current. The primary current and the zener current are not in the same phase because of the influence of the magnetizing current.

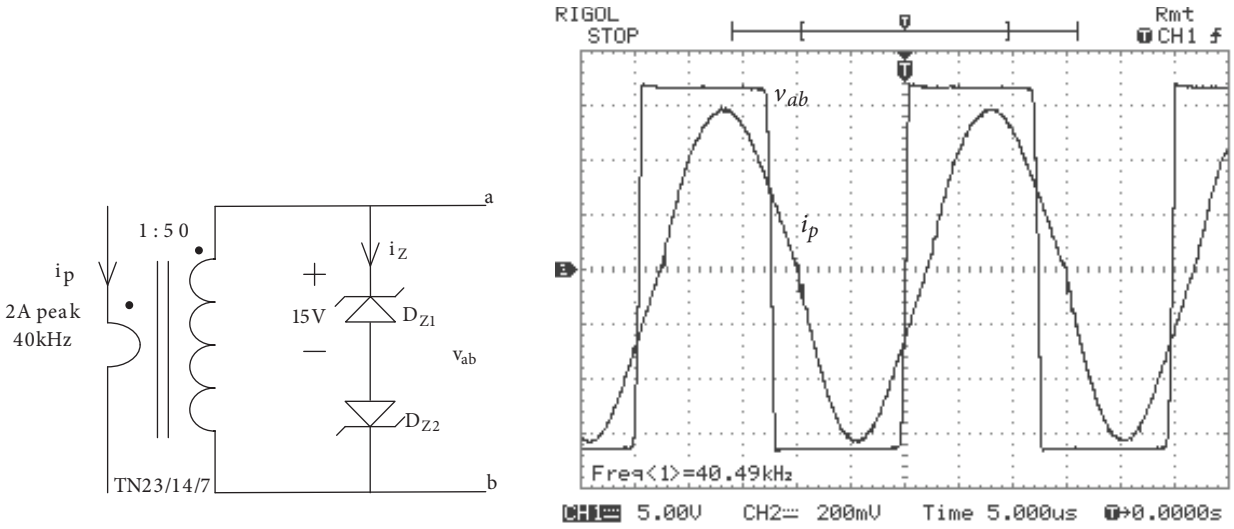

(a) (b) CH1: v_{ab} , CH2: i_p

Figure 6. a) Experimental study circuit and b) experimental results.

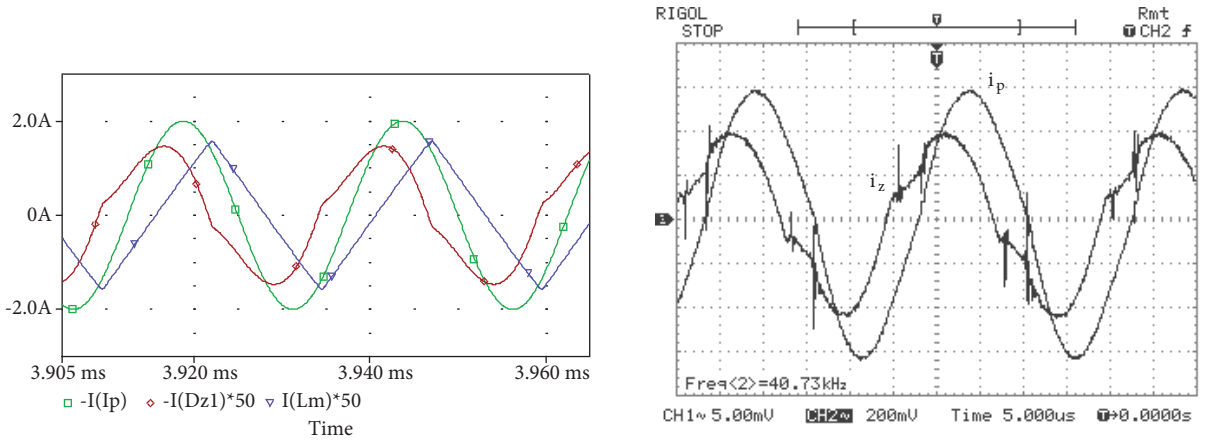

(a) (b)

Figure 7. The primary and zener diode currents: a) simulation and b) experiment (CH1: i_z , CH2: i_p).

The calculated and simulated peak magnetizing current results are given in Table 4.

Table 4. The calculated and simulated magnetizing peak current results.

	$I_{m,peak}\,(mA)$	
n	Calculated	Simulation
40	48	48.8
45	38	38.63
50	31	31.27

The magnetizing current increases as the number of secondary turns decreases.

3.2. Effect of the magnetizing current on the driving voltage

As seen in Figure 4c, one of the advantages of obtaining the CT linear model is the ability to investigate the magnetizing current in the circuit. For this reason, in a self-oscillating converter, the influence of magnetizing inductance on the driving voltage can be examined and the working characteristic of the system can be observed. For this purpose, the parametric simulation circuit was designed, as shown in Figure 8. A sinusoidal current source with the peak value of 50 mA at 40 kHz is used here.

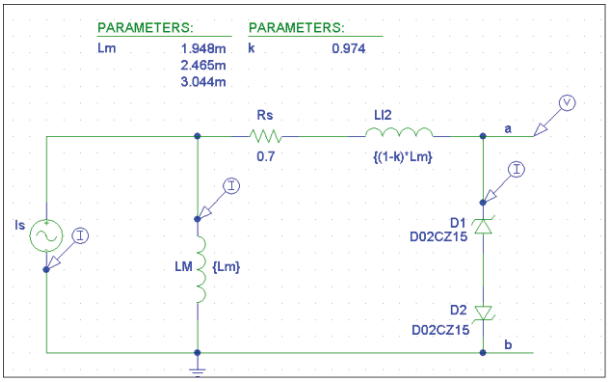

Figure 8. The parametric simulation circuit of the CT linear model.

The magnetizing inductance values of the circuit are chosen according to Table 2. The change in the magnetizing current and the driving voltage can be seen simultaneously in Figure 9. As the magnetizing current increases, the phase difference between the driving voltage and the secondary current increases.

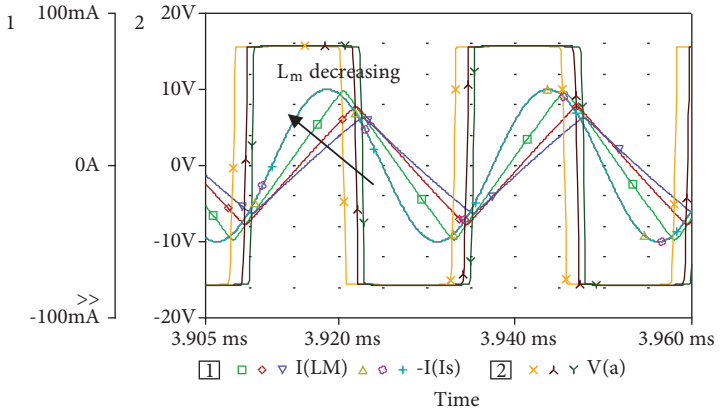

Figure 9. Effect of the magnetizing current on the driving voltage.

3.3. Effect of secondary current on the driving voltage

According to Eq. (10), the critical peak value for the secondary current becomes 30.798 mA in the CT where the secondary windings have 50 turns. The effect of the secondary current on the driving voltage for the chosen number of windings is examined in the simulation circuit in Figure 10. The critical current value calculated according to Eq. (10) is taken into consideration; therefore, in the parametric simulation, a current source with 25- and 35-mA peak values is used to provide currents below and above the critical secondary current.

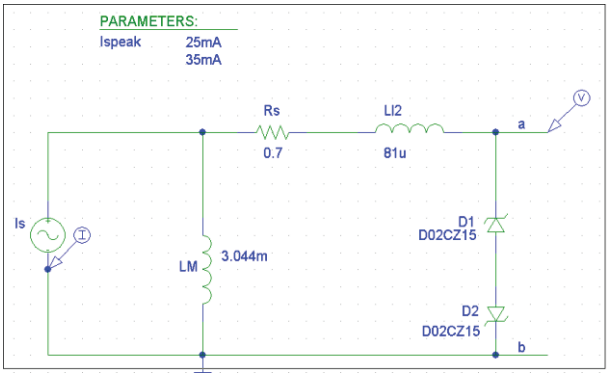

Figure 10. The simulation circuit for different secondary currents.

Figures 11a and 11b show the simulation results of the driving voltage for below and above the critical secondary current.

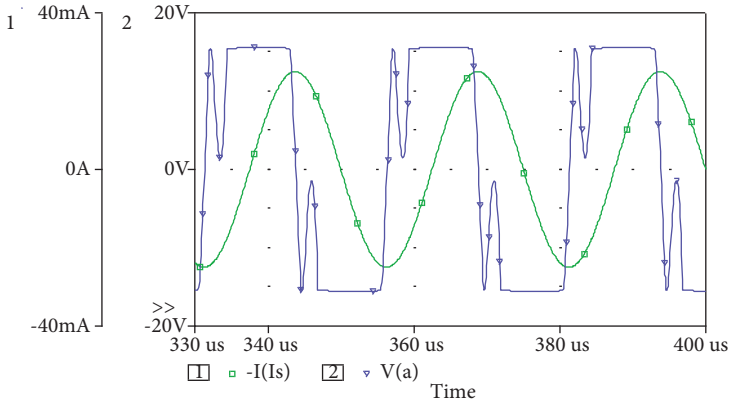

(a)

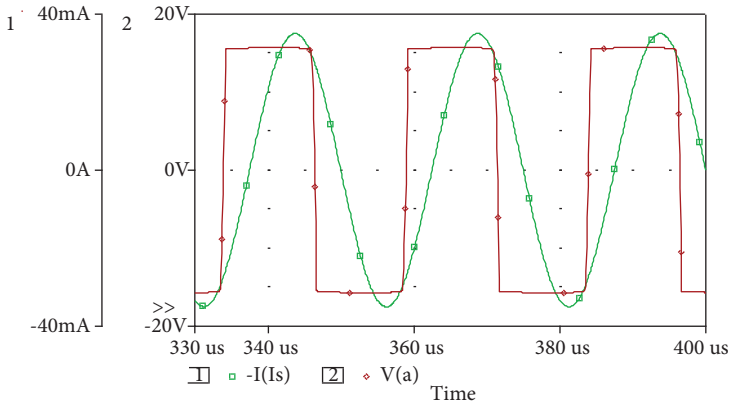

(b)

Figure 11. The simulation results for different secondary currents.

Figures 12a and 12b are the experimental results showing the change in the driving voltage for below and above the critical secondary current.

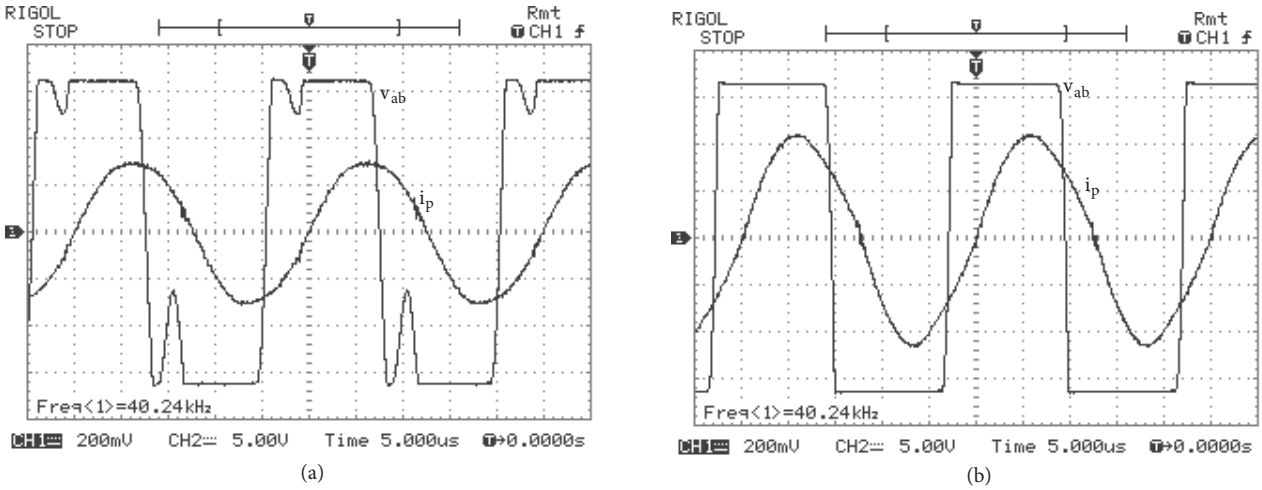

Figure 12. Experimental results for different secondary currents ($I_s = I_p/50$).

According to the results of the application and simulation, the driving voltage gets deformed below the approximate critical secondary current values and the deviation between the primary current and the driving voltage increases.

The differences between the simulated and the experimental results occur for the following reasons: the zener diode model used in the simulation is not exactly the same as the model used in the application. Additionally, an ideal core cannot be used in the transformer, so the core does not have a linear characteristic.

4. Conclusions

One of the application areas for CTs is the drive circuit for self-oscillating converters. In the self-oscillating drive circuit, the CT's magnetizing current and the zener diode voltage affect the driving voltage and switching frequency. In this study, the linear circuit model of the CTs was designed. The results of the CT calculated from the electrically equivalent circuit and the linear model were compared with the results obtained from the simulation and application. Hence, the effect of the transformer's magnetizing current could be examined. For different turn ratios, the effect of the magnetizing current and the secondary current on the driving voltage can be seen in the linear model simulation, where the parametric simulation method is used. As the magnetizing current increases, the phase error between the driving voltage and the secondary current increases. The driving voltage with a square wave form cannot be obtained for values below the critical secondary current. As the number of secondary windings decreases, the phase of the current gets delayed when compared to the driving voltage. This situation affects the phase angle of the self-oscillating converters. The circuit model brings the advantage of testing the conditions for different magnetizing inductance and secondary current conditions of the self-oscillating driver.

References

[1] K.L. Williams, "Fundamentals of current transformer", Electrical Electronics Insulation Conference, pp. 23–25, 1995.

[2] H. Kifune, Y. Hatanaka, "Resonant frequency tracking control by using one CT for high frequency inverter", EPE 13th European Conference on Power Electronics and Applications, pp. 1–7, 2009.

[3] G.S.S. Chau, S. Ziegler, H.H.C. Iu, H. Daniyal, "Experimental verification of the linear current transformer model", Australasian Universities Power Engineering Conference, pp. 1–6, 2008.

[4] A.R.A.M. Makky, H. Abo-Zied, F.N. Abdelbar, P. Mutschler, "Design of the instrument current transformer for high frequency high power applications", 12th International Middle-East Power System Conference, pp. 230–233, 2008.

[5] A.R. Seidel, F.E. Bisogno, H. Pinheiro, R.N. do Prado, "Self-oscillating dimmable electronic ballast", IEEE Transactions on Industrial Electronics, Vol. 50, pp. 1267–1274, 2003.

[6] C. Liu, L. Ping, W. Chuanbing, C. Hu, Z. Zhang, "Analysis of the voltage feedback self-oscillating electronic ballasts", 40th IAS Annual Meeting. Conference Record of the Industry Applications Conference, Vol. 4, pp. 2753–2757, 2005.

[7] M. Ponce-Silva, R. Mateos, E. Flores, D. Balderrama, A. Claudio, "Driver for 2.5 MHz self-oscillating electronic ballast designed with descriptive function", IEEE Power Electronics Specialists Conference, pp. 2857–2860, 2008.

[8] N. Kondrath, M.K. Kzimierczuk, "Bandwidth of current transformers", IEEE Transactions on Instrumentation and Measurement, Vol. 58, pp. 2008–2016, 2009.

[9] A.R. Seidel, F.E. Bisogno, R.N. do Prado, "A design methodology for a self-oscillating electronic ballast", IEEE Transactions on Industry Applications, Vol. 43, pp. 1524–1533, 2007.

[10] R. Lin, Y.F. Chen, Y.Y. Chen, "Design consideration of self-oscillating full-bridge electronic ballast for metal halide lamp at 2.65 MHz operating frequency", IEEE Energy Conversion Congress and Exposition, pp. 1591–1597, 2010.

[11] P. Lopes, M.F. da Silva, R.A. Pinto, R.N. do Prado, A.R. Seidel, "Universal input voltage self-oscillating electronic ballast with feedforward control", IEEE Industry Applications Society Annual Meeting, pp. 1–5, 2009.

[12] L.R. Nerone, "A mathematical model of the class D converter for compact fluorescent ballasts", IEEE Transactions on Power Electronics, Vol. 10, pp. 708–715, 1995.

[13] D.C. King, "Toroidal coil winding and construction techniques", Proceedings of the Electrical Insulation Conference and Electrical Manufacturing Expo, pp. 337–340, 2005.

[14] Philips, TN23 / 14 / 7 Datasheet, 1999.